Abbreviated title: **Hypoxia in temperate headwaters**

Title: **Hypoxia is common in temperate headwaters and driven by hydrological extremes**

Jacob S. Diamond[1*], Laurent Valette[1], Rémi Recoura-Massaquant[1], Arnaud Chaumot[1], Gilles Pinay[2], Jay Zarnetske[3], Florentina Moatar[1]

[1]RiverLy, INRAE, Centre de Lyon-Grenoble Auvergne-Rhône-Alpes, France 69100

[2]Environnement, Ville & Société (EVS UMR5600), Centre National de la Recherche Scientifique (CNRS), Lyon, France

[3]Department of Earth and Environmental Sciences, Michigan State University, East Lansing, Michigan; USA

[*]**Correspondence to**: jacob.diamond@inrae.fr; +330636134204 ; RiverLy, INRAE, 5 rue de la Doua, Villeurbanne, France, 69100

Abstract

Hypoxia, or dissolved oxygen (DO) at low enough levels to impair organisms, is a particularly useful indicator of the health of freshwater ecosystems. However, due to limited sampling in headwater networks, the degree, distribution, and timing of hypoxia events are not known across the vast majority of most river networks. We thus sought to clarify the extent of hypoxia in headwater networks through three years of instrumentation of 78 sites across eight temperate, agricultural watersheds. We observed broadly distributed hypoxia, occurring 4% of the time across 51 of the 78 sites over 20 months. The hypoxia was driven by three mechanisms: storm events, drying, and rewetting, with drying as the most common driver of hypoxia (55% of all hypoxic event types). Drying induced hypoxia was most severe in smaller streams (Strahler orders ≤ 3), whereas storm events preferentially induced hypoxia in the larger streams (Strahler orders 3–5). A large diversity in DO trajectories towards hypoxia depended on hydrologic event type, with subsequent expected differences in mortality profiles of a sensitive species. Predictive models showed the most vulnerable sites to hypoxia were small streams with low slope, particularly during hot, low discharge periods. Despite variation among hypoxic events, there was remarkable similarity in the rate of DO drawdown during hypoxia events (ca. 1 mg O_2 L^{-1} d^{-1}). This drawdown similarity may be a useful rule-of-thumb for managers, and we hypothesize that it is a signal of increasing downstream network-scale oxygen demand. Overall, we posit that hypoxia is likely a common feature of most headwater networks that often goes undetected. Headwater hypoxia may become more common under increasingly dry conditions associated with climate and water resource management changes, with important implications for biological communities and biogeochemical processes.

keywords: drought, hypoxic, drying, storms, rewetting, dissolved oxygen, temperature

Introduction

Low oxygen concentrations in fresh and salt waters are common and increasing in both spatial and temporal extent around the world (Breitburg et al., 2018; Jenny et al., 2016). While mechanisms driving low oxygen concentrations, or hypoxia, are well documented in lakes and coastal areas, it is less well documented or understood in river networks that are often assumed to be oxic. Hypoxia is known to lead to mortality (Rabalais et al., 2010 and references therein), mobilize chemically reduced contaminants into the water column (Saup et al., 2017), and exacerbate greenhouse gas emissions (Bastviken et al., 2004). Sparked both by these growing environmental concerns and by a proliferation of rather inexpensive, accurate, and rugged dissolved oxygen sensor technology (Rode et al., 2016), interest is mounting to understand the spatiotemporal distributions of hypoxia in river waters (Dutton et al., 2018; Garvey et al., 2007). Yet, of these river systems, headwater stream hypoxia dynamics are still the least understood (Blaszczak et al., 2019; Carter et al., 2021; Gómez-Gener et al., 2020; Pardo and García, 2016).

Hypoxia in river systems can arise from a number of interacting processes linked to high levels of respiratory or reductive processes somewhere in the hydrologic network. Broadly speaking, we can define five underlying drivers of hypoxia, each of which is associated with amplified respiratory processes. In no particular order, there are: 1) excess N and P input leading to eutrophication, particularly in lakes/estuaries (Breitburg et al., 2018; Smith and Schindler, 2009), 2) point source pollution (Mallin et al., 2006; McConnell, 1980), 3) storms, which can bring in low O_2 groundwater (Carter et al., 2021) or oxygen demanding substances (Dutton et al., 2018; Kerr et al., 2013; Whitworth et al., 2012), 4) drying (Pardo and García, 2016; Tramer, 1977), and 5) rewetting, which may stimulate microbial activity (Acuña et al., 2005). These varied drivers, in particular storms, drying, and rewetting, may have distinct hypoxic signatures that are important for the survival of biota.

The low primary productivity relative to respiratory processes (Diamond et al., 2021; Vannote et al., 1980) and increased likelihood for drying of headwater streams (Godsey and Kirchner, 2014) suggests their trends towards longer and more frequent hypoxia events. Still, most studies on stream hypoxia focus on humid climate streams and rivers larger than Strahler order 2; less is known regarding the smaller order streams of headwater networks (Bishop et al., 2008) that typically experience greater flow intermittence (Gómez-Gener et al., 2020). These headwaters are the network capillaries connecting land to the river network and they physically dominate total stream length and benthic area of river networks (Benstead and Leigh, 2012; Strahler, 1957). By not studying this dominant portion of river networks, there may be a large underestimation of the total extent of freshwater hypoxia.

Hypoxic episodes may become more common in headwaters under increased climate-driven drought frequency and intensity (Dai, 2013; Samaniego et al., 2018), especially in agricultural areas already experiencing irrigation-induced water deficits (Elliott et al., 2014). The link between hydrologic extremes and hypoxia further suggests that headwaters may exhibit disproportionately more hypoxia than downstream reaches, as they typically have greater hydrologic responses to climate and land use change. Moreover, small stream drying patterns typically lead to the formation of pools and hydrologic disconnection, i.e., “pooling” (Godsey and Kirchner, 2014; Stanley et al., 1997) with understudied effects on subsequent heterogeneity in oxygen and community physiological effects.

We addressed these research gaps by studying the oxygen regimes in agricultural headwater rivers to assess the environmental conditions leading to headwater hypoxia, and the subsequent degree of hypoxia throughout the networks. We hypothesized that hypoxic events would arise under drying, storm, and rewetting conditions, but that hypoxia would be greatest

and most common in the smallest streams due to their increased risk for drying and pooling. We further evaluated the potential impact of hypoxia on aquatic animal communities using the modeled mortality response of the amphipod *Gammarus fossarum,* a sentinel organism of water quality in stream ecosystems (Chaumot et al., 2015; Kunz et al., 2010) known for its sensitivity to dissolved oxygen (Hervant and Mathieu, 1995; Maltby, 1995; Meijering, 1991). We hypothesized that the model organisms would exhibit a mortality threshold response to lower DO, which we could use as a way to set an ecologically relevant definition of hypoxia in our stream networks.

Methods

Study area

We instrumented 78 sites, spanning Strahler orders 1–5 across eight catchments in France: 1) Coise, 2) Loise, 3) Toranche, 4) Mare, 5) Lignon, 6) Ardières, 7) Vauxonne, and 8) Yzeron (Figure 1, Table 1). These catchments were monitored for hypoxia between 3 July 2019 to 15 October 2021 (except winters from November 1–February 28) The first five catchments (Coise–Lignon) are primarily agricultural headwater catchments of the Loire River basin, and were instrumented from July 2019–October 2020, with 4, 11, 16, 8, and 3 sites in orders 1–5, respectively. In these catchments, granite and gneiss lithology at upper catchment boundaries gradually gives way to thick alluvium with clay and sand at catchment outlets in a flat basin known as the Forez plain. The geology in the upper reaches prevents substantial aquifer storage leading to regular drying. Topography is characterised by rolling hills with successions of plateaus separated by steep slopes. Climate in these catchments is continental, with mean annual temperature of 11°C (range during measurement period = 0.0–34.3°C) and mean annual precipitation of 800 mm.

106 The Ardières and Vauxonne catchments are adjacent, but just across the regional
107 drainage divide and are tributaries of the Sâone River, which itself is a tributary of the Rhône
108 River. From 8 March 2021 to 14 October 2021, we instrumented 2, 6, 8, and 3 sites of Strahler
109 order 2, 3, 4, and 5 respectively. These two catchments drain a hilly landscape of vineyards (32%
110 land cover) exposed to pesticides (Montuelle et al., 2010). Soil is sandy loam on a shallow
111 Hercynian crystalline bedrock. Climate is temperate with a mean annual air temperature of
112 17.1ºC (-2.1–35.2°C) and mean annual precipitation is 940 mm, with intense summer
113 thunderstorms. The combination of climate, soil and steep slopes (up to >30%) is conducive to
114 infiltration and sub-surface lateral flow (Gouy et al., 2021).
115 The last catchment, the Yzeron is a direct tributary of the Rhône River, draining a steep
116 agricultural and forested landscape composed of magmatic and metamorphic (granite, gneiss,
117 schist) bedrock that leads downstream to a semi-urban/urban zone with Quaternary fluvio-glacial
118 and glacial deposits. From 08 March 2021 to 15 October 2021, we instrumented 2, 3, 6, 6, and 1
119 sites from Strahler orders 1–5, respectively. The climate is a mix of continental/Mediterranean
120 with mean annual temperature 13.8°C (-5.5–28.1°C) and mean annual rainfall 800 mm
121 (Gnouma, 2006), which predominately occurs in spring and autumn. The hydrological regime is
122 pluvial with low flows in summer and floods in autumn and spring. Road and storm sewages
123 designed for flood mitigation allow rapid transport of urban runoff to downstream channels of
124 the Yzeron.

Table 1. Characteristics of the Loire and Rhône tributaries' catchments and summary of their hydrochemistry from grab samples, mean±sd (n).

Variable	Loire					Rhône		
	Coise	**Loise**	**Toranche**	**Mare**	**Lignon**	**Ardières**	**Vauxonne**	**Yzeron**
N sites	11	20	3	4	4	15	3	18
Area (km^2)	6.1–350	0.8–132	54.7–76.1	61.9–233	62.1–664	3.6–142	6.6–46.0	0.8–59.4
Alt.† (m)	344–619	337–627	338–377	352–422	330–360	199–389	227–228	197–731
Q^{*} ($m^3\ s^{-1}$)	0.17	0.13	0.06	0.34	1.11	0.59	0.19	0.10

pH	7.8±0.2 (40)	7.5±0.4 (123)	7.7±0.4 (27)	7.8±0.2 (35)	7.6±0.3 (43)	7.5±0.1 (91)	7.8±0.1 (17)	7.6±0.3 (107)
SpC** ($\mu S\ cm^{-1}$)	296±129 (71)	315±255 (156)	320±82 (33)	193±79 (49)	136±57 (59)	145±45 (166)	238±59 (32)	322±124 (195)
DOC†† ($mg\ L^{-1}$)	4.6±1.1 (24)	4.3±1.6 (73)	7.0±1.4 (13)	7.0±1.6 (20)	5.1±1.6 (26)	3.3±0.9 (125)	ND	6.7±2.9 (78)
NO_3–N ($mg\ L^{-1}$)	2.3±1.9 (24)	2.2±2.1 (73)	2.4±2.3 (13)	1.2±0.6 (20)	0.9±0.6 (26)	2.2±1.8 (88)	2.0±1.6 (17)	2.1±1.3 (78)
PO_4^{3-}–P ($mg\ L^{-1}$)	0.12±0.12 (24)	0.07±0.07 (73)	0.11±0.1 (13)	0.08±0.05 (20)	0.08±0.06 (26)	0.1±0.1‡ (45)	ND	0.08±0.07 (78)

†altitude in meters above NGF IGN69 datum
*interannual median at the outlet during sampling period
**specific conductance at 25ºC
††dissolved organic carbon
‡estimated from Montuelle et al. (2010)
ND = no data

125

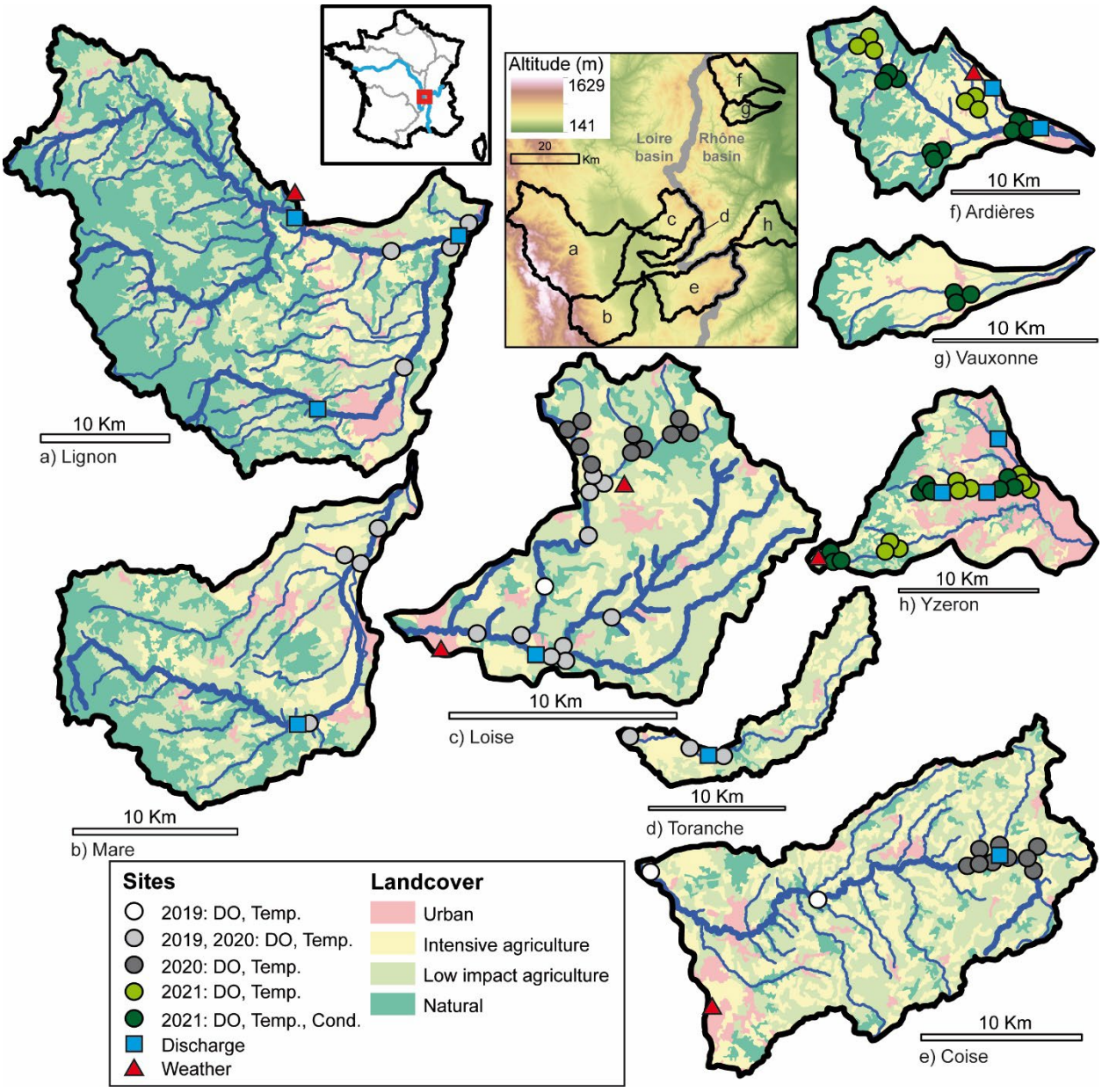

Figure 1. Map of instrumented study sites with points indicating sensor placement and monitoring duration.

Data collection and processing

We monitored the sites for dissolved oxygen (DO; mg L^{-1}) and stream temperature (°C) for variable periods between July 2019 and October 2021, but not during winter (November–February; Figure 1). At each site, DO and stream temperature were measured every 15 minutes with an in-situ sensor (HOBO U26-001, Onset Computer Corporation, Massachusetts, USA)

instrumented with a copper anti-biofouling guard. At 12 sites in 2020 and 18 sites in 2021, we installed conductivity sensors (HOBO U24-001, Onset Computer Corporation, Massachusetts, USA). We cleaned DO and conductivity sensors with a toothbrush every two weeks to remove biofouling. Prior to deployment, we lab-calibrated DO sensors with both 100% water-saturated air and with sodium sulphite for 0% saturation. Conductivity sensors were calibrated based on field measurements obtained with a calibrated handheld probe (Pro Plus, YSI Inc., Ohio, USA) at the beginning and end of each two-week measurement period per manufacturer instructions. We also measured DO and temperature with the calibrated handheld probe at each field visit to check for sensor drift and develop corrections as needed. We placed sensors in the middle of the water column, and as close to the thalweg as possible. As streams began to dry, we vertically repositioned sensors to keep them submerged and continuously capture stream DO and prevent loss of data.

Across all sites, we measured DO and stream temperature at 15-minute intervals for a total of 1,687,776 measurements. The quality controls applied to all DO data prior to analysis are described in detail in Diamond et al. (2021). Briefly, we 1) averaged 15-minute data to hourly resolution to reduce file sizes and processing time, 2) removed data that were extremely noisy, collected in dry conditions, or otherwise of suspect quality, and 3) corrected for minimal sensor drift. For data that passed quality control (n_{DO}=380,161), we calculated hourly DO saturation (DO_{sat}) and specific conductance.

Storm, drying, and rewetting events

We observed three environmental events conducive to hypoxia across our sites: 1) storms, 2) drying, and 3) rewetting. Each of these environmental events were identified according to the following definitions. First, we classified storm events as a doubling of baseflow (Carter et al., 2021), with storms at least 24 hours apart counting as separate events. We used the

functions *high.spells* and *baseflow* (based on a Lyne-Hollick recurvise digital filter) from the *hydrostats* R package (Bond, 2022) to determine these events. Through sensitivity analyses, we determined these criteria to accurately and reproducibly capture each distinct event in the observed discharge time series. To determine storm effects on DO, we examined the three days before the storm peak flow and the week following the peak flow (Carter et al., 2021).

Second, to classify distinct drying events, we relied on a combination of sensor data, field observations, and discharge data. Ideally, accurate local discharge or stage data should characterize these events, but the large number of sites precluded continuous measurement at each location, and there is a well-known problem with low-flow accuracy from local stream network gages (Zimmer et al., 2020). Hence, to indicate dry periods, we used the observation that DO sensors read near-saturation and experience air-temperature-like fluctuations when they are out of the water. These dry-period DO sensor observations are directly supported by 1) concurrent conductivity measurements (reading near 0 $\mu S\ cm^{-1}$), 2) field observations of dry stream beds, and 3) near-zero or zero-flow measurements of discharge at local discharge stations. Therefore, these moments (i.e., when sensors are out-of-water) represent the end-points of our drying periods. We then determined the beginning points of our drying periods by extending the end-point backwards in time to a point when specific discharge measurements exceeded the 10% percentile, using the *low.spell.lengths* function from *hydrostats*.

Third, rewetting events were demarcated by typically rapid and large reductions in temperature, and increases in conductivity of stream water after dry periods. These moments were also associated with measured rainfall events and concomitant discharge responses, so we have high confidence in the start time of rewetting events. The length of a rewetting event lasted either until the stream dried again (see above), or until discharge exceeded the 10% percentile.

To avoid over-counting drying events, we did not consider the drying after rewetting to be a drying event as defined above unless the discharge exceeded the 10% percentile before re-drying after rewetting.

Hypoxia evaluation

In this study, we defined instantaneous hypoxia conditions to occur in the stream water when DO is less than 3 mg O_2 L^{-1}. This instantaneous hypoxia level was selected for three primary reasons: 1) it is national threshold value for "bad" ecological potential of water quality in France (Ministère chargé de l'écologie, 2019), 2) it appears to be a threshold for mortality in the biological indicator species, *Gammarus fossarum* (Fig. S1), and 3) measurements of DO concentrations are less uncertain and require fewer assumptions than estimates of DO percentage saturation, although this metric is still commonly used (e.g. 50%, Carter et al., 2021). Some regulatory agencies define coastal hypoxia as < 2 mg L^{-1} (NSTC, 2003) though evidence suggests freshwater biota experience chronic toxicity below 5 mg L^{-1} (Saari et al., 2018). Overall, there is no single definition for hypoxia, and different numeric thresholds may be appropriate for the regulation or study of specific impacts (in mg L^{-1} or % saturation).

As there is no single assessment of hypoxia and its impacts, we evaluated the degree of hypoxia in several ways. Apart from simply calculating total hours and percentage of hypoxia within and across sites, we also delineated continuous hypoxic events (with up to a 2-hour gap of DO > 3 mg L^{-1}), taking into account their lengths, and periodicity, and the diel distributions of hypoxia. We further calculated rates of DO drawdown leading to hypoxia during storm, drying, and rewetting events by fitting linear regressions through daily minima (Carter et al. 2020). Finally, we attempted to identify simple predictors of hourly hypoxia (i.e., binary: hypoxic or oxic) with logistic regression and classification trees (R package rpart; Therneau and Atkinson, 2022). Potential predictors of DO conditions measured included stream habitat of the DO sensor

(pool, riffle, or run; visually assessed), hourly stream temperature, daily specific discharge of the catchment, reach slope, Strahler order, distance from the source, and altitude. Data were highly skewed towards oxic conditions, so we balanced the data with combined over- and under-sampling using the R package *ROSE* (Lunardon et al., 2014). We split the dataset into training (70%) and testing (30%) data for model building and validation, respectively.

Prediction of gammarid mortality during hypoxic events

To connect observed hypoxia events with hypoxia physiological response for stream biota, we modeled *Gammarus fossarum* ("gammarid") mortality using measured DO concentrations from contrasting hypoxic event types as input to a General Unified Threshold model of Survival (GUTS) (Jager et al., 2011). The GUTS toxicokinetic-toxicodynamic model, based on bioassay survival data, is regularly used in prospective hazard assessment of pesticides and fluctuating concentrations of toxic chemicals (Ockleford et al., 2018). GUTS quantifies mortality rate evolution based on the internal concentrations of hazardous compounds in organisms, which are controlled both by uptake rates and internal contaminant elimination rates (Baudrot et al., 2018). We adapted GUTS to include hypoxic stress instead of toxic stress by considering the DO deficit below an arbitrary value of 12 mg L^{-1} as the stressor input metric (instead of contaminant concentration). Using the web-interface MOSAIC (https://mosaic.univ-lyon1.fr/guts) (Charles et al., 2018), we calibrated the GUTS model with an experimental dataset of gammarid mortality in laboratory conditions under different constant levels of DO deficit (Recoura-Massaquant et al., 2022). We used the reduced individual tolerance version of the model (GUTS-RED-IT), which assumes a log-logistic distribution of sensitivity threshold among individuals. The calibration experiment consisted of monitoring mortality over a five-day laboratory exposure of 300 male organisms of homogenous body size (~10 mm) to 10 constant nominal DO concentration conditions (8, 6, 5, 4, 3.5, 3, 2.5, 2, 1.5 and 1 mg L^{-1}, respectively),

with three replicates of 10 individuals per concentration condition (Fig. S1). DO deficits were obtained by bubbling N_2 gas through water columns. All detailed experimental data are available from the open access data repository Recherche Data Gouv (Recoura-Massaquant et al. 2022). We then used the calibrated GUTS-RED-IT model to estimate potential mortality responses under observed hypoxic scenarios from three storm events and five drying events.

Results

Degree of hypoxia across sites

Overall, we observed 16,781 hours of hypoxia (DO < 3 mg L^{-1}), an average of 4.4% of all site hourly measurements from 2019–2021. Hypoxia occurred at 51 of 78 sites for at least one hour of hypoxia, and at 37 sites for at least 1% of the time. The greatest degree of hypoxia was in 2019, accounting for 9.2% of all measurements that year, followed by 2020 with 6.2%, and 2021 with 1.3%. Note that in 2021, in addition to being a wetter year (Fig 2b), the sites changed from the Loire to the Rhône basin (Fig. 1). Among catchments, the Toranche experienced the most hypoxia (12.9% or 2,335 hours), and the Vauxonne the least (0.3% or 57 hours; Table S1). In general, hypoxia was spatially heterogeneous, but drying tended to synchronize hypoxia within catchments. For example, in late July 20, when most sites in the Loise catchment were almost dry, sites ranging 4.2–31.4 km^2 (7 out of 16 sites) exhibited hypoxia at the same time before drying.

Across our sites, we observed correlations between the degree of monthly hypoxia and stream temperature (Fig. 2a) and specific discharge (Fig. 2b). Hence, hypoxia was greatest in summer months (Fig. 2d) when temperatures were greatest and discharge was lowest. There were negligible differences in hypoxia rates between night and day, although solar noon was the least likely time to observe hypoxia (Fig. 2c). Mean hypoxic duration was 10 hours, and while this did not vary over time (Fig. 2d), there was two orders of magnitude variation across events

253 (range=1–210 hours). In general, differences in degree of hypoxia among Strahler orders were
254 marginal (Table 2), and did not correspond to downstream trends ($p > 0.05$ for all linear fits).
255 Still, Strahler order 1 exhibited the lowest degree of hypoxia for all metrics.

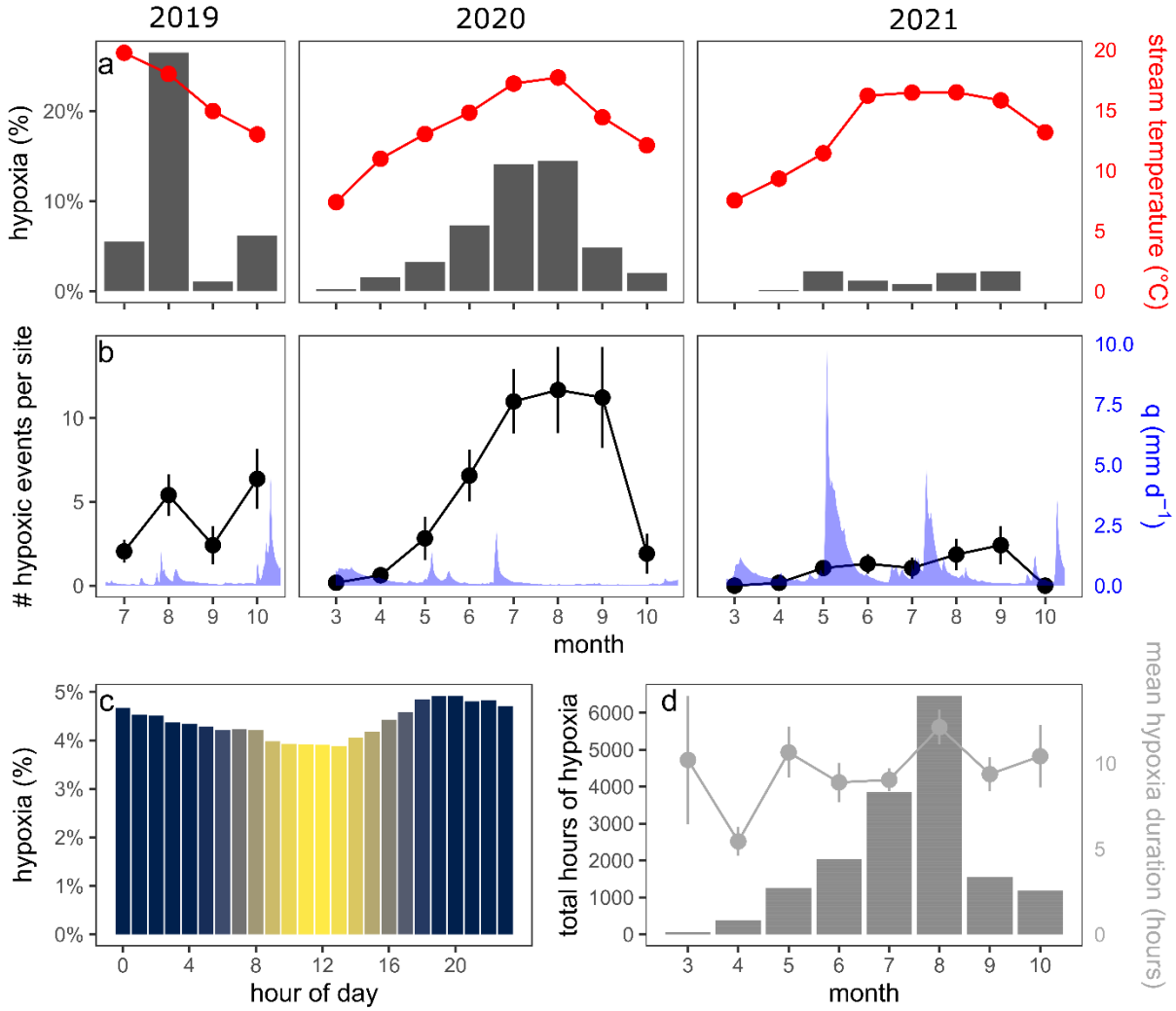

256

257 **Figure 2.** Time series of hypoxia metrics. a) Monthly percentage of measurements that were
258 hypoxic (bars) with mean monthly across-site stream temperature (red) for 2019–2021 (columns
259 for a and b). b) Mean monthly number of unique hypoxic events aross sites (black, vertical bars
260 are standard errors) and mean daily specific discharge (blue) across gaging stations. c) Hourly
261 percentage of measurements that were hypoxic across sites and years, with lighter colors

indicating daylight hours. d) Total hours of hypoxia (bars) and the mean duration of hypoxia (grey, vertical bars are standard errors) across sites and years by month.

Table 2. Hypoxia summary statistics by Strahler order, mean±sd when given.

Strahler order	Total hypoxia (hours)	Percentage of time hypoxic* (%)	Unique hypoxia events** (n)	Event length† (hours)	Time between events†† (days)	Night hypoxia‡ (%)
1	786	3.1	34	8±6	3.0±11.3	51%
2	3180	4.9	44	9±11	5.5±18.8	49%
3	7778	5.1	73	10±13	9.3±43.1	48%
4	3015	3.0	37	10±10	13.7±45	49%
5	2022	5.6	27	14±17	9.9±31.5	50%

*Total hours of hypoxia divided by total hours of DO measurements × 100
** Event defined as at least one hour of DO < 3 mg L^{-1}; events continue with up to 2-hour gap in hypoxia
†Event length begins at time of first hypoxia and continues until hypoxia ends, with up to 2-hour gap in hypoxia
††The time between hypoxic events
‡The percentage of total hypoxia that was measured at night, where night is defined as <200 μmol m^{-2} s^{-1} PAR

Storm events

We recorded 152 storm events across the 13 discharge gages with an average storm pulse length of 2.6±4.2 days (mean±sd; range = 1 hour–22.1 days), leading to 776 site-events. Of those site-events, 107 resulted in at least one hour of hypoxia. For 131 of the 669 site-events without hypoxia, there was no change in DO mean or variance after the storm peak (ANOVA and t-tests of 5 days before and after; $p>0.01$), whereas 414 of them exhibited an increase in DO, but no change in DO diel range. Storm events resulting in hypoxia occurred predominately in higher order sites, with 87% in orders 3–5, and 62% in orders 4–5.

DO trajectories following storm events were highly variable (Fig. S2). Of the storms that induced hypoxia, it took a median of 41 hours (53±48 hours) after peak discharge to become hypoxic, ignoring sites that were hypoxic prior to the storm. This is the amount of time for DO to drop between 8.0 and 3.3 mg L^{-1} when using the median and mean rates of DO decrease (Fig. 3b). Sites stayed hypoxic for a median of 7 hours (20±32 hours) after first becoming hypoxic.

There were 48 events where peak discharge rapidly induced oxic conditions to previously hypoxic sites, but oxic conditions rarely lasted for more than a few days (Fig. 3a). These event types were spread across 25 sites and every Strahler order and habitat. There were few obvious predictors of the effect of a particular storm event on changes to DO, with time since last storm event, baseflow before storm event, and storm pulse magnitude having no predictive power (Fig. 3c).

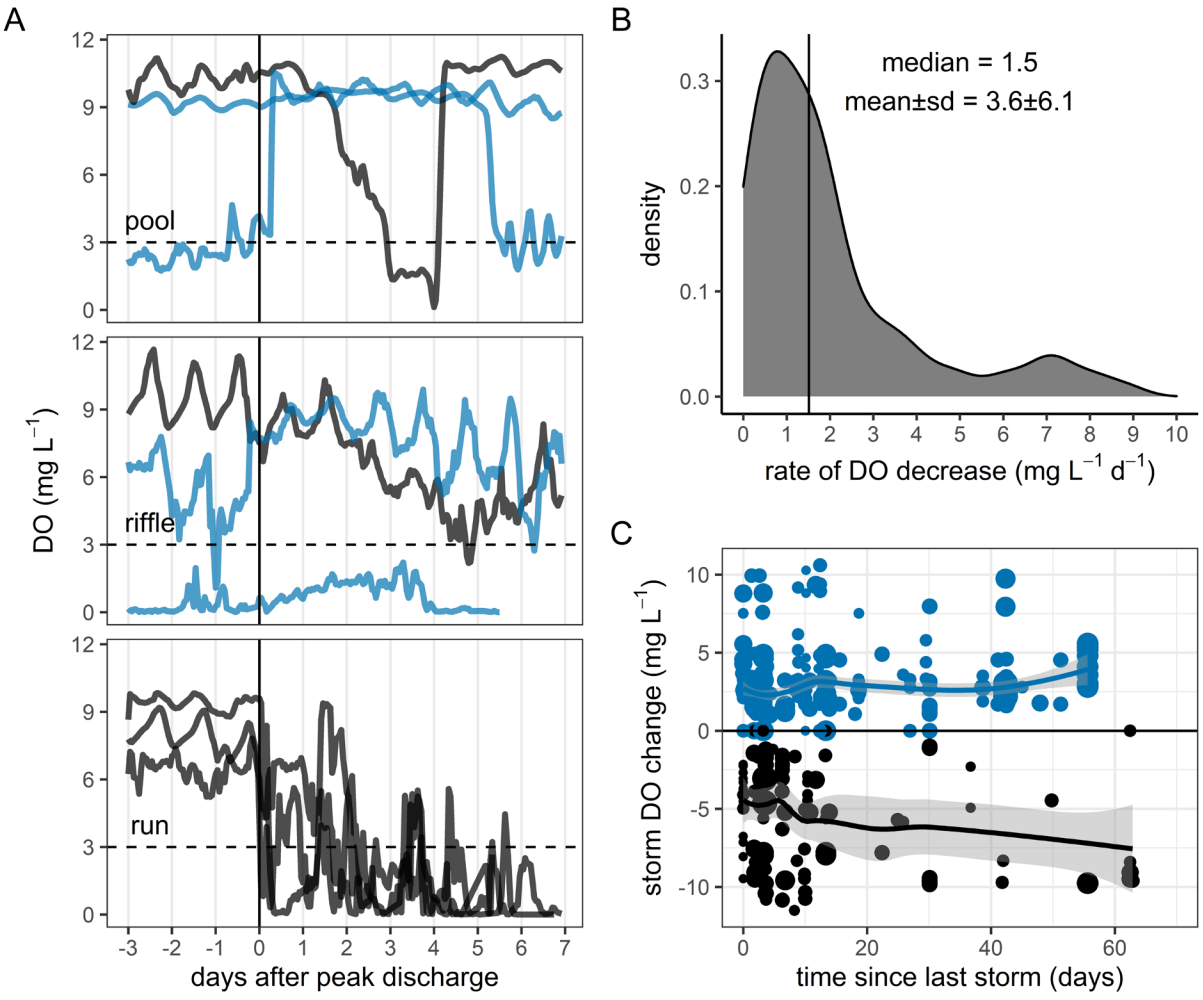

Figure 3. Summary of storm event effects on DO. A) three different storm events for each of three different habitat types (pool, riffle, run) with colors indicating whether DO increased (blue) or decreased (black) after the storm event. Dashed line indicates hypoxia and vertical line

indicates peak discharge. B) Distribution of DO decreases (black events in panel A) across all events that led to a decrease in DO. C) Comparison of change in DO (colors as in A) as a function of time since the last storm, with the point size indicating the magnitude of the storm pulse. LOESS lines with 95% confidence intervals are shown.

Drying

Across all 13 stream gages in the study area, dry conditions were recorded 86 times with a mean dry duration of 6.7±11.2 days (range = 8 hours – 86 days). Flow was lowest in 2019 and 2020 (Fig. 2b). In the Loire basin, the Loise, Coise, and Toranche catchments experienced zero-flow for 2%, 2%, and 24% of days in 2019, and 11%, 11%, 29% in 2020. Average dry durations for those catchments were 1, 1, and 4.5 days in 2019, and 1, 1, and 80 days in 2020. In the Rhône basin, sites in the Yzeron catchment in 2021 also experienced drying 1.5–4.6% of the time, with average site dry durations of 4.9–11.8 days. Using our criteria to determine if a sampling site was dry, we estimate that 23 of 78 sites became dry at least once. Within those 23 sites, we observed 60 distinct drying events (2.6±1.5 events per site). The remaining results refer to these hypoxic drying events (Fig. 2a).

Drying was the most common hydrologic driver of hypoxia, accounting for 55% of all hypoxic events. The mean hypoxia duration during drying was 6.2 hours (range = 1–55 hours); the greatest durations occurred in Strahler order 2 (mean = 9.3±9.5 hours). The smaller Strahler orders (1–3) were twice as likely to become hypoxic during drying than to remain oxic, and for Strahler order 1 drying events always resulted in hypoxia. The mean decrease in daily DO minima was 1.3 mg L^{-1} d^{-1} (Fig. 4b), with relatively little variation (IQR = 0.6–1.5 mg L^{-1} d^{-1}). This decrease in DO was not concomitant with increases in stream temperature, which did not exhibit increasing trends with drying ($p>0.05$). Once drying began, it took 3.8±2.9 days for sites to become hypoxic (IQR = 1.8–4.8 days). We observed increases ($p < 0.05$) in DO diel ranges

over drying periods in 12 instances (18% of hypoxic drying events), with a mean increase of 0.7±0.5 mg L^{-1} d^{-1}. Apart from Strahler order (Fig. 4c), there were no clear predictors of a site to become hypoxic during drying or on how long it would stay hypoxic.

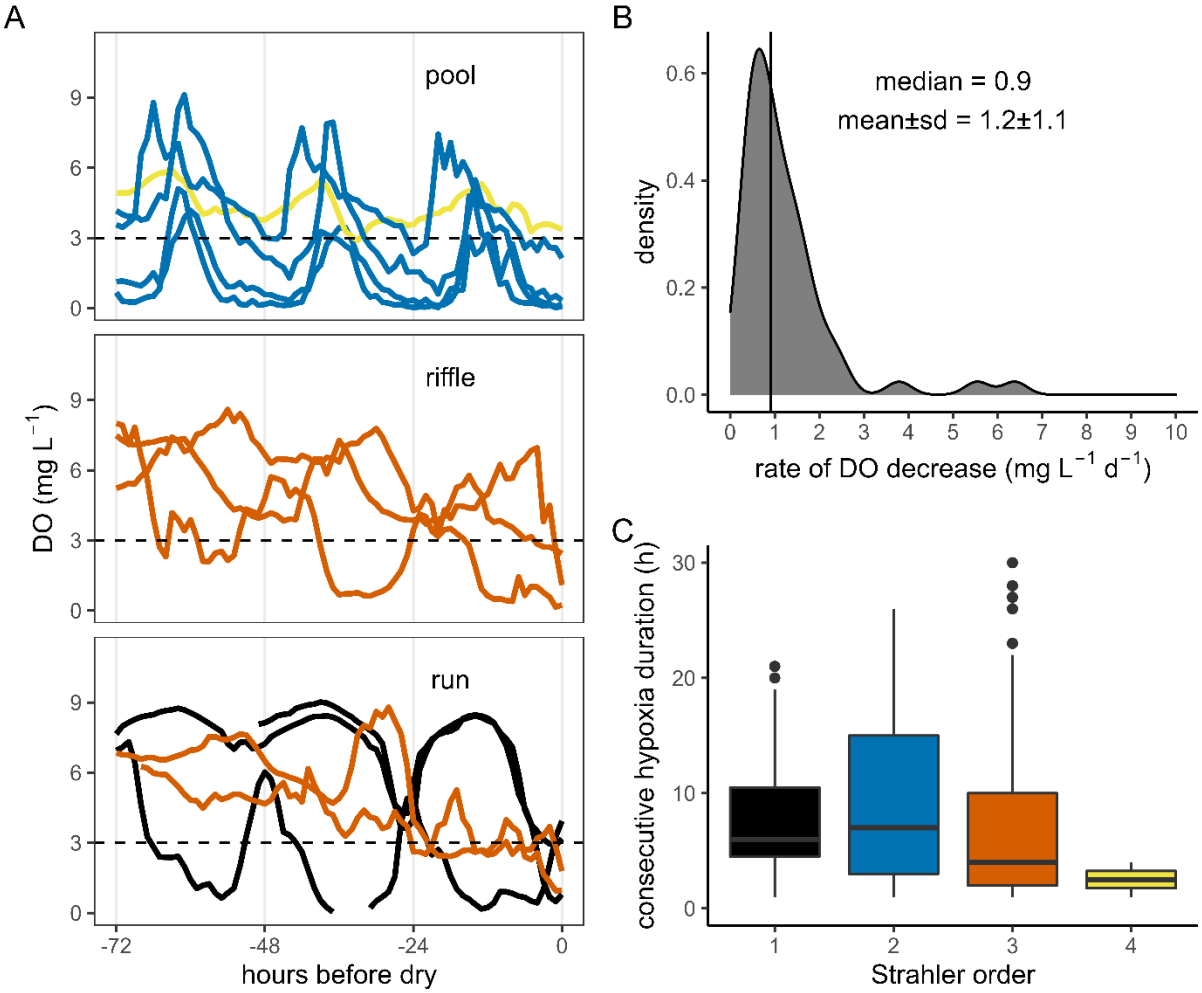

Figure 4. Summary of drying hypoxia events. A) Three-to-four different drying events for each of three different habitat types (pool, riffle, run) with colors indicating Strahler order; dashed line indicates hypoxia. B) Distribution of DO decreases across all events. C) Length of consecutive hypoxia (colors as in A) as a function of Strahler order.

Rewetting

There were 314 rewetting events according to our criteria with 46 of these events leading to at least one hour of hypoxia. These events occurred across 27 of 78 sampling sites. There was a mean duration of 6±13 days of dry conditions before rewetting, and sites went through an average of 4.9±4.7 drying and rewetting cycles. Rewetting led to more decreases than increases in DO (Fig. 5b). When only considering negative changes, the mean decrease in DO was -1.0±1 mg L^{-1} d^{-1} (median = -0.7 mg L^{-1} d^{-1}). Apart from the fact that there were no riffle rewetting events that led to hypoxia (Fig. 5a), there were no other obvious controls on DO changes after rewetting, e.g. dry period duration or previous number of dry periods before rewetting (Fig. 5c).

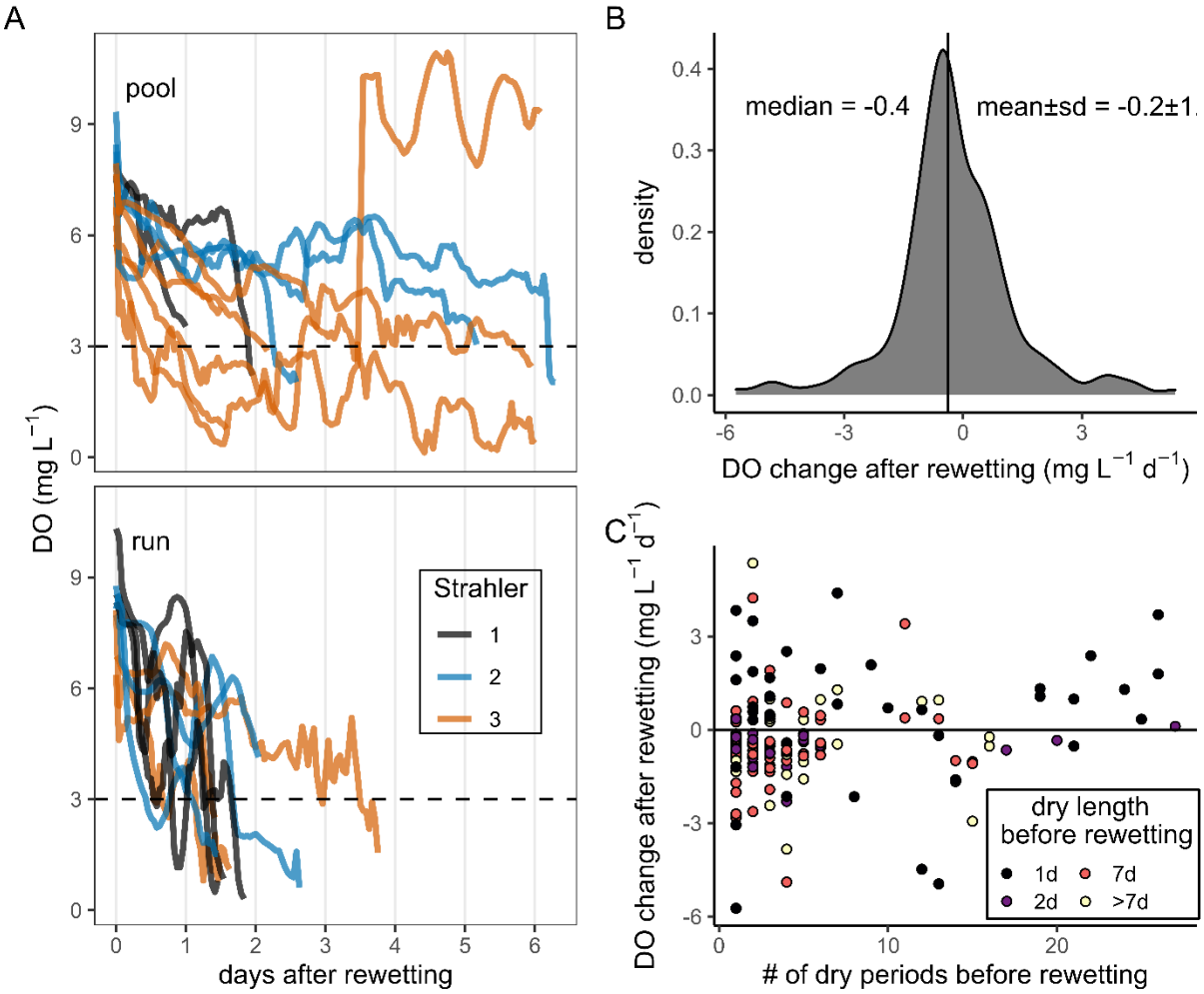

Figure 5. Summary of rewetting event effects to DO. A) Different rewetting events leading to hypoxia for each of two different habitat types (pool and run; riffles did not experience rewetting hypoxia) with colors indicating Strahler order; dashed line indicates hypoxia. B) Distribution of DO changes across all events, vertical line indicates median. C) DO change after rewetting as a function of the number of dry periods before rewetting and the dry period duration (colors).

Predicting hypoxia

A classification tree was able to predict instances of hypoxia across a training dataset with an accuracy of 81% (c-statistic = 0.79, sensitivity = 0.67, specificity = 0.82). Notably, the resulting 10-node tree predicted hypoxic events with probability = 0.79 for periods with stream temperature > 11ºC, specific discharge < 0.014 mm d^{-1} (ca. 1-10 L s^{-1} for these catchments), and Strahler order ≤ 3 (Fig. S3). The highest probability of hypoxia (p=0.86) was observed for the same temperature conditions, but for discharge > 0.014 mm d^{-1}, and reach slopes 0.042–0.054 m m^{-1}. The lowest probabilities for hypoxia were under cold-water conditions (temperature < 11 ºC) and high slope conditions (slope ≥ 0.054 m m^{-1}). The variable importance for the classification tree were temperature = 34, slope = 32, specific discharge = 18, Strahler = 10, and habitat = 6. Similar variable importance was observed for a regression tree on DO (Fig. S4).

Given that discharge and temperature were the most important continuous variables in predicting hypoxia and DO at our sites, we used them as predictors in a logistic regression for hypoxia. The model (Table 3) performed relatively poorly (Fig. S5) with a pseudo R^2=0.10 (McFadden, 1987) and accuracy 63% (c-statistic = 0.66, sensitivity = 0.69, and specificity =0.63), especially when compared with the classification tree. Holding temperature constant, the odds of hypoxia decreased by 15% for each unit increase in ln(q), whereas by holding discharge constant, the odds of hypoxia increased by 19% for each °C increase.

Table 3. Logistic regression results for probability of hypoxia*

Coefficients	Estimate	SE	z-value	p-value
Intercept	-3.0	0.02	-151	<0.0001
ln(q)**	-0.16	0.00	-71	<0.0001
temperature	0.17	0.00	-131	<0.0001

*$\hat{p} = \frac{\exp(b_0+b_1\ln(q)+b_2 temp)}{\exp(1+b_0+b_1\ln(q)+b_2 temp)} = \log\frac{p(hypoxia)}{1-p(hypoxia)}$

**daily specific discharge [mm d^{-1}]

354

355 *Gammarid mortality patterns*

356 The laboratory experiments revealed a gammarid mortality threshold response to DO at 3
357 mg L^{-1} (Fig. S1). The predictions of the calibrated GUTS model based on our field data for storm
358 and drying events thus follow this threshold, with mortality occurring when DO < 3 mg L^{-1} (Fig.
359 6). There was a clear difference in mortality profiles between drying and storm hypoxic events,
360 with a staircase shape for the drying, and a more continuous and abrupt shape for storms. The
361 staircase mortality under drying is due to the marked diel DO oscillations that allow oxic
362 recovery periods during the day. Hence, the time between the start of hypoxia and the quasi-
363 extinction of the population of individuals (e.g. 95% dead) is much shorter for storms than for
364 drying events. Specifically, storm events achieved quasi-extinction in less than two days for the
365 three storm events considered, whereas it took at least three days for the drying events, with one
366 drying event not crossing 50% mortality (Fig. 6b).

367 During drying, successive mortality events were triggered for successively lower DO
368 thresholds. This is explained by the Individual Tolerance assumption in GUTS model, where the
369 population loses the most sensitive individuals first, but only the most tolerant ones when the
370 stress conditions worsen. This is most apparent for the longer drying event (blue line on Fig. 6b)
371 with a first large event of mortality at day 9 when DO concentrations reach 3 mg L^{-1}, followed

by a phase without mortality between days 10–15 while DO still fluctuates in the same concentration range. A second event of mortality occurs only when DO < 2 mg L^{-1}.

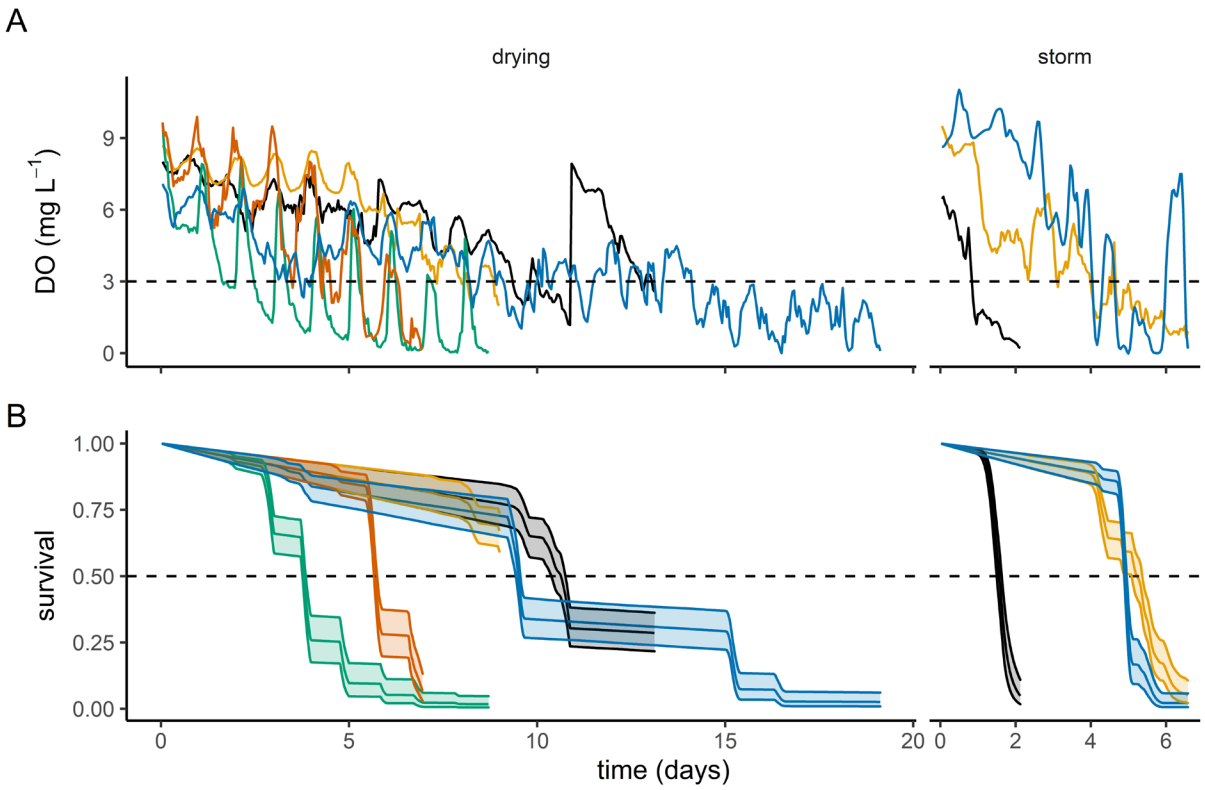

Figure 6. Summary of GUTS model results for gammarid survival under hypoxia driven by drying and storms. A) Time series of DO concentrations for eight different hypoxic events (five drying and three storms), colored by individual event. B) Time series of gammarid survival (1=100% population survives, 0 = complete mortality) with 95% confidence intervals in shade. Dashed lines indicate hypoxia and 50% mortality in A and B, respectively. Note different x-axis lengths for storms and drying.

Discussion

Hypoxia is abundant in space and time in headwaters

Hypoxia was temporally common over the growing season across our study area, with a surprisingly even spatial distribution across watersheds and Strahler orders. This ran counter to

our hypothesis that hypoxia would occur preferentially in the smallest streams (e.g., Strahler order < 3), and there was moreover little difference in degree of hypoxia among sites (Table 2). Equally surprising was that there were marginal differences between night and day hypoxia at the study- or Strahler order-level (Fig. 1, Table 2; cf. Carter et al. 2021), suggesting that when it occurs, it spans full night and day periods. Still, hypoxia was slightly more common in the early evening, suggesting most grab-sample monitoring approaches are underestimating its extent. Spatially, although we sampled Strahler order 3 (n=29) at twice the rate of order 2 (n=14) and five times the rate of order 1 (n=6), normalized hypoxia metrics (Table 2) still indicate parity among these smallest orders with the larger orders 4 (n=21) and 5 (n=8). Although common across Strahler orders, hypoxia occurrence was spatially stochastic and created patches of oxic and hypoxic areas that were separated as a function of local characteristics unquantified here (Fig. S3, Table 3). This is an important nuance to consider when modeling at larger scales: e.g., drying does not uniformly induce hypoxia.

The unexpected commonality of hypoxic conditions in this study supports growing observations of apparent non-eutrophication related hypoxia across watersheds of varying size, climate, geology, and land use (Blaszczak et al., 2019; Carter et al., 2021; Gómez-Gener et al., 2020). Thus, hypoxia may be an overlooked aspect of catchment hydrochemistry, with implications for nutrient processing and community dynamics (Pardo and García, 2016).

Hydrologic events induce variable hypoxia trajectories

Hypoxia events exhibited distinct characteristics–from initiation to recovery–that depended on hydrologic event type. The most rapid hypoxia trajectories evolved under storm events (Fig. 3a) and rewetting (Fig. 5a). Both storm and rewetting events exhibited dynamic DO changes (Fig. 3b, Fig. S2, Fig. 4b), which were not explained by several common sense factors such as size of the storm pulse, time since last storm or last rewetting cycle (Fig. 3c, Fig. 4c),

409 stream habitat, or Strahler order. However, we note that pools were generally slower to reach
410 hypoxia than runs under rewetting events (Fig. 4a), likely due to their greater water volume and
411 oxygen mass. Overall, we noted the emergence of several archetypal storm pulse DO behaviors,
412 including no changes, immediate drops, slow drops, and a peak of high DO aligning with the
413 storm peak followed by gradual drawdown to hypoxia. Point source inflows of low DO or high
414 oxygen-demanding substances may explain the rapid DO drop storm archetype observed here
415 (Dutton et al., 2018). The latter archetype of a DO peak followed by drawdown was the most
416 commonly observed in a low-gradient, humid catchment with an order of magnitude higher
417 discharge (Carter et al., 2021), hinting at a common driver. We suggest this could be a
418 hydrologic mechanism.

419 Storm peaks likely drive high gas exchange, leading to rapid oxygenation, but afterwards
420 we hypothesize that increased soil respiration after storm events (Lee et al., 2004; Sponseller,
421 2007) entails low DO water to the stream after the storm peak. Soil respiratory processes may
422 reduce the DO in hillslope or nearby riparian groundwater, especially as rising groundwater
423 intercepts greater proportions of soil carbon (Li et al., 2021; McGuire and McDonnell, 2010) as
424 noted in dissolved organic carbon export patterns (e.g., Diamond and Cohen, 2018; Zarnetske et
425 al., 2018). Such soil respiration pulses typically last less than 48 hours (Lee et al., 2004) and
426 would likely arrive in baseflow after the peak, roughly aligning with the timeframe of our
427 observations. Thus, the slower DO drawdown archetype may be explained by mobilization of
428 “old” water lateral inflows during storm events that push low DO water into the stream channel
429 at a volume that replaces any pre-storm in-channel DO (Brown et al., 1999; Buttle, 1994; Klaus
430 and McDonnell, 2013).

In contrast to storms and rewetting, drying events consistently exhibited a gradual DO drawdown towards hypoxia. These drawdowns were often associated with large diel swings in DO, particularly for pools and runs (Fig. 3a). Such swings would often lead to temporary relief from hypoxia during daylight hours, unless primary productivity and gas exchange were too low to match respiratory demand. It was during drying periods that the stream network as a whole was the most likely to undergo synchronous hypoxia (cf. Diamond et al. 2022), although individual site trajectories towards hypoxia were highly heterogeneous. Dry periods thus compound hydrologic stress on organisms with low oxygen stress, and likely represent critical periods for metacommunity development (Sarremejane et al., 2017).

Hypoxia induced potential mortality of an indicator species

The combination of hypoxia mode, magnitude, and temporal characteristics controlled the extent of organismal mortality or survival. Storm (or rewetting) events induced classic pulse disturbances with rapid mortality, whereas drying was more akin to a stress disturbance with gradual mortality (Fig. 6) (Bender et al., 1984). As such, drying press disturbances may leave possibilities for gammarids to find modes of survival during daytime hypoxia alleviations due to DO increases from primary productivity. This is in contrast to storms, which cause more intense and rapid crashes in DO. Hence, it is not just the presence of hypoxia, but the trajectory into and out of it that likely matters to biota.

We note here that the coupling of seasonal population phenology and hypoxia is likely a strong control of subsequent drops in gammarid densities. For instance, we observed most hypoxia during summer, but population models demonstrate that this is the least sensitive period of gammarid adult mortality (Coulaud et al., 2014), suggesting some inherent population-level resilience. Conversely, while there is limited evidence on embryo or egg response to hypoxia, it

seems plausible that these life phases may be more sensitive than the adults tested here, implying major demographic consequences in summer (Geffard et al 2010; Coulaud et al 2014).

Despite our findings of a clear risk of hypoxia-induced mortality events for the gammarid populations, these modeled outcomes need to be supported by empirical studies. For example, additional lab manipulations with variable DO concentrations, and in-situ exposure studies will allow more nuanced study of how DO dynamics affect populations. Moreover, such studies would permit direct testing of the Individual Tolerance approach used in this work. Our choice for using the Individual Tolerance model, which assumes that there are differences in sensitivity among individuals, derives purely from its better fit with the lab data. The hypothesis of the existence of tolerant and sensitive individuals could be tested in the lab by applying, for example, two successive hypoxia events to evaluate if the mortality levels shift at the second event. The likely existence of less sensitive individuals would imply inheritance of genetic fortitude against hypoxia such that future generations may be more tolerant of increasingly lower levels of DO.

Difficulty predicting hypoxia

We did not find a simple, robust way to predict hypoxic events based on site level habitat, geomorphic, hydrologic, or thermal conditions. These are all relatively easy to measure attributes of streams that are often incorporated as fundamental parts of many stream ecosystem and hydrological models, so seeing no strong predictive power in them presents a challenge for easy modeling of hypoxia in headwaters. Our best model suggests that hypoxia tends to occur under high temperature, low slope, low discharge, and small Strahler order conditions, but this model still had very limited predictive success (67% true positive rate). These best predictors tend to align with other stream DO work, particularly the small slope (Carter et al., 2021) and low discharge-small Strahler order conditions (Gómez-Gener et al., 2020). Within these conditions,

and under storm event conditions, we did not observe clear predictors of the degree of hypoxia (e.g., hypoxia duration)–we could only assess the likelihood for some level of hypoxia to occur. Hence, there are missing fundamental controls in our array of predictors that can distinguish these hypoxic events. Perhaps the lack of geomorphologic complexity across sites limited the gradient of predictors able to explain the variance in hypoxia, but the diversity of hypoxic trajectories and responses even within a narrow range geographic area suggests the need for alternative hypotheses on hypoxia controls. We surmise that local hydrology–especially lateral inflows, point sources, and hyporheic exchange, which were poorly constrained here–is likely a strong predictor of hypoxia dynamics at the scale of small headwater streams.

Consistent oxygen drawdown under various conditions

Despite the fact that we observed a range of hypoxic trajectories under storms, drying, and rewetting events, the median rate of drawdown leading to hypoxia was remarkably similar across events and sites—approximately 1 mg O_2 L^{-1} d^{-1}. We suggest that this may imply an increasing downstream network-scale oxygen demand (i.e., "ecosystem respiration" [g O_2 m^{-2} d^{-1}]). For this pattern to emerge, oxygen demand should increase downstream at roughly the same rate as depth increases (e.g., in proportion to $d \approx Q^{0.3}$; Raymond et al. 2012). This is because depth increases the volume of water and thus the mass of oxygen at a given concentration: mass flux must therefore increase to reduce the concentration by a consistent magnitude at increasing volumes. This downstream increase in demand may only become apparent when the balancing DO controls of primary production and gas exchange are minimal. Indeed, under storm and recession conditions, primary production is often reset to zero due to scouring and turbidity (O'Donnell and Hotchkiss, 2022; Uehlinger, 2000; Uehlinger and Naegeli, 1998) leading to respiration dominance. Under drying conditions, pool formation and low flow reduce gas exchange (Stanley et al., 1997) and reduced replenishment of upstream nutrients for primary

502 production, lead to respiration dominance of the DO signal. Interestingly, previous efforts
503 observed weak-to-no longitudinal pattern of ecosystem respiration in this region, although DO
504 proxies for ecosystem respiration revealed strong downstream increases (Diamond et al., 2021).
505 The observation of similar DO drawdown under varying conditions is at the very least
506 useful as a rule-of-thumb for managers when wanting to estimate time-until-hypoxia. For
507 instance, assuming typical summer conditions with daily DO minima around 7 mg L^{-1}, one could
508 expect the first instances of hypoxia in about four days under drought conditions. Moreover, we
509 observed similar durations of hypoxia (ca. 7-hours) among drying and storm events, implying an
510 additional rule-of-thumb when estimating or modeling hypoxia-induced mortality of sensitive
511 species. Importantly, drying-induced hypoxia is likely to be exacerbated upon rewetting,
512 suggesting a compounded effect of drought on DO quality. Also useful to managers and
513 researchers is that our results demonstrate that low Strahler order streams, despite being
514 historically overlooked for hypoxia, will be the most likely to undergo hypoxia in drought
515 conditions. In other words, these river network capillaries should be hotspots for future
516 investigation of hypoxia and its biological effects.

517 **Conclusions**

518 We observed regular hypoxic conditions across eight temperature agricultural networks
519 with varying land use, geology, and hydrology. Although common, hypoxia occurrence was
520 spatially stochastic and created patches of oxic and hypoxic reaches. Hypoxia across 78 sites
521 spanning Strahler orders 1–5 was driven by storms, drying, and rewetting, with drying being the
522 dominant mechanism. Models based on our field data indicated that storms and drying events are
523 pulse- and press-disturbances, respectively, whose distinct hypoxia signals induce corresponding
524 mortality profiles in sensitive species. We conclude that the DO trajectory into and out of
525 hypoxia drives mortality patterns with implications for metacommunity structure and

development. Despite difficulty in predicting the degree and specific occurrences of hypoxia, we showed that hypoxia is most likely to occur in small, low slope streams, under high temperature and low discharge conditions, but that storm-induced hypoxia is preponderant to higher order streams. Regardless of the hydrologic driver of hypoxia, we observed a remarkably consistent daily drawdown in DO of 1 mg L^{-1}, suggesting a downstream increase in oxygen demand, and a useful rule-of-thumb for managers. Overall, we conclude that hypoxia is a regular and increasingly common occurrence in headwater networks with the potential to be a strong control on biogeochemistry and biological communities, meriting its continued study.

Author Contributions

JD–conceptualization, design, sampling, analysis, writing

FM–conceptualization, design, analysis, writing

GP– conceptualization, design, sampling, analysis, writing

LV–sampling, analysis, writing

AC–sampling, analysis, writing

RR–sampling, analysis, writing

JZ–analysis, writing

Acknowledgments

This project was supported by The Loire-Bretagne Water Agency and the Rhône-Méditerranée-Corse Water Agency. JD was also supported by the EUR H2O'Lyon, French ANR-17- EURE-0018 grant. JZ contributions were partially supported by US NSF awards (1846855, 1916567) and a fellowship from the Collegium - Lyon, Institute for Advanced Study. We thank Pierre Martinache and Nicolas Delorme for technical support with lab tests and field work, and Sandrine Charles (UMR 5558 Lyon 1) for her advice on modelling gammarid mortality. We also

549 thank Michèle Gailleton and Paul Courbière for their very kind hospitality to access field sites
550 and to develop experiments on their properties.

551 **Literature Cited**

552 Acuña, V., Muñoz, I., Giorgi, A., Omella, M., Sabater, F., Sabater, S., 2005. Drought and
553 postdrought recovery cycles in an intermittent Mediterranean stream: structural and
554 functional aspects. Journal of the North American Benthological Society 24, 919–933.
555 https://doi.org/10.1899/04-078.1
556 Bastviken, D., Cole, J., Pace, M., Tranvik, L., 2004. Methane emissions from lakes: Dependence
557 of lake characteristics, two regional assessments, and a global estimate. Global
558 Biogeochemical Cycles 18. https://doi.org/10.1029/2004GB002238
559 Baudrot, V., Veber, P., Gence, G., Charles, S., 2018. Fit Reduced GUTS Models Online: From
560 Theory to Practice. Integrated Environmental Assessment and Management 14, 625–630.
561 https://doi.org/10.1002/ieam.4061
562 Bender, E.A., Case, T.J., Gilpin, M.E., 1984. Perturbation Experiments in Community Ecology:
563 Theory and Practice. Ecology 65, 1–13. https://doi.org/10.2307/1939452
564 Benstead, J.P., Leigh, D.S., 2012. An expanded role for river networks. Nature Geosci 5, 678–
565 679. https://doi.org/10.1038/ngeo1593
566 Bishop, K., Buffam, I., Erlandsson, M., Fölster, J., Laudon, H., Seibert, J., Temnerud, J., 2008.
567 Aqua Incognita: the unknown headwaters. Hydrol. Process. 22, 1239–1242.
568 https://doi.org/10.1002/hyp.7049
569 Blaszczak, J.R., Delesantro, J.M., Urban, D.L., Doyle, M.W., Bernhardt, E.S., 2019. Scoured or
570 suffocated: Urban stream ecosystems oscillate between hydrologic and dissolved oxygen
571 extremes. Limnology and Oceanography 64, 877–894.
572 Bond, N., 2022. hydrostats: Hydrologic Indices for Daily Time Series Data. R package version
573 0.2.9.
574 Breitburg, D., Levin, L.A., Oschlies, A., Grégoire, M., Chavez, F.P., Conley, D.J., Garçon, V.,
575 Gilbert, D., Gutiérrez, D., Isensee, K., Jacinto, G.S., Limburg, K.E., Montes, I., Naqvi,
576 S.W.A., Pitcher, G.C., Rabalais, N.N., Roman, M.R., Rose, K.A., Seibel, B.A.,
577 Telszewski, M., Yasuhara, M., Zhang, J., 2018. Declining oxygen in the global ocean and
578 coastal waters. Science 359, eaam7240. https://doi.org/10.1126/science.aam7240
579 Brown, V.A., McDonnell, J.J., Burns, D.A., Kendall, C., 1999. The role of event water, a rapid
580 shallow flow component, and catchment size in summer stormflow. Journal of Hydrology
581 217, 171–190. https://doi.org/10.1016/S0022-1694(98)00247-9
582 Buttle, J.M., 1994. Isotope hydrograph separations and rapid delivery of pre-event water from
583 drainage basins. Progress in Physical Geography: Earth and Environment 18, 16–41.
584 https://doi.org/10.1177/030913339401800102
585 Carter, A.M., Blaszczak, J.R., Heffernan, J.B., Bernhardt, E.S., 2021. Hypoxia dynamics and
586 spatial distribution in a low gradient river. Limnology and Oceanography.
587 Charles, S., Veber, P., Delignette-Muller, M.L., 2018. MOSAIC: a web-interface for statistical
588 analyses in ecotoxicology. Environ Sci Pollut Res 25, 11295–11302.
589 https://doi.org/10.1007/s11356-017-9809-4
590 Chaumot, A., Geffard, O., Armengaud, J., Maltby, L., 2015. Chapter 11 - Gammarids as
591 Reference Species for Freshwater Monitoring, in: Amiard-Triquet, C., Amiard, J.-C.,

592 Mouneyrac, C. (Eds.), Aquatic Ecotoxicology. Academic Press, pp. 253–280.
593 https://doi.org/10.1016/B978-0-12-800949-9.00011-5
594 Coulaud, R., Geffard, O., Coquillat, A., Quéau, H., Charles, S., Chaumot, A., 2014. Ecological
595 Modeling for the Extrapolation of Ecotoxicological Effects Measured during in Situ
596 Assays in Gammarus. Environ. Sci. Technol. 48, 6428–6436.
597 https://doi.org/10.1021/es501126g
598 Dai, A., 2013. Increasing drought under global warming in observations and models. Nature
599 Clim Change 3, 52–58. https://doi.org/10.1038/nclimate1633
600 Diamond, J.S., Pinay, G., Bernal, S., Cohen, M.J., Lewis, D., Lupon, A., Zarnetske, J., Moatar,
601 F., 2022. Light and hydrologic connectivity drive dissolved oxygen synchrony in stream
602 networks. Limnology and Oceanography 00, 1–14.
603 https://doi.org/10.1002/lno.12271
604 Diamond, J.S., Bernal, S., Boukra, A., Cohen, M.J., Lewis, D., Masson, M., Moatar, F., Pinay,
605 G., 2021. Stream network variation in dissolved oxygen: Metabolism proxies and
606 biogeochemical controls. Ecological Indicators 131, 108233.
607 https://doi.org/10.1016/j.ecolind.2021.108233
608 Diamond, J.S., Cohen, M.J., 2018. Complex patterns of catchment solute–discharge relationships
609 for coastal plain rivers. Hydrological Processes 32, 388–401.
610 https://doi.org/10.1002/hyp.11424
611 Dutton, C.L., Subalusky, A.L., Hamilton, S.K., Rosi, E.J., Post, D.M., 2018. Organic matter
612 loading by hippopotami causes subsidy overload resulting in downstream hypoxia and
613 fish kills. Nat Commun 9, 1951. https://doi.org/10.1038/s41467-018-04391-6
614 Elliott, J., Deryng, D., Müller, C., Frieler, K., Konzmann, M., Gerten, D., Glotter, M., Flörke,
615 M., Wada, Y., Best, N., Eisner, S., Fekete, B.M., Folberth, C., Foster, I., Gosling, S.N.,
616 Haddeland, I., Khabarov, N., Ludwig, F., Masaki, Y., Olin, S., Rosenzweig, C., Ruane,
617 A.C., Satoh, Y., Schmid, E., Stacke, T., Tang, Q., Wisser, D., 2014. Constraints and
618 potentials of future irrigation water availability on agricultural production under climate
619 change. Proceedings of the National Academy of Sciences 111, 3239–3244.
620 https://doi.org/10.1073/pnas.1222474110
621 Garvey, J.E., Whiles, M.R., Streicher, D., 2007. A hierarchical model for oxygen dynamics in
622 streams. Canadian Journal of Fisheries and Aquatic Sciences 64, 1816–1827.
623 Gnouma, R., 2006. Aide à la calibration d'un modèle hydrologique distribué au moyen d'une
624 analyse des processus hydrologiques: application au bassin versant de l'Yzeron. Thèse de
625 doctorat, INSA Lyon.
626 Godsey, S.E., Kirchner, J.W., 2014. Dynamic, discontinuous stream networks: hydrologically
627 driven variations in active drainage density, flowing channels and stream order.
628 Hydrological Processes 28, 5791–5803.
629 Gómez-Gener, L., Lupon, A., Laudon, H., Sponseller, R.A., 2020. Drought alters the
630 biogeochemistry of boreal stream networks. Nat Commun 11, 1795.
631 https://doi.org/10.1038/s41467-020-15496-2
632 Gouy, V., Liger, L., Ahrouch, S., Bonnineau, C., Carluer, N., Chaumot, A., Coquery, M., Dabrin,
633 A., Margoum, C., Pesce, S., 2021. Ardières-Morcille in the Beaujolais, France: A
634 research catchment dedicated to study of the transport and impacts of diffuse agricultural
635 pollution in rivers. Hydrological Processes 35, e14384. https://doi.org/10.1002/hyp.14384

Hervant, F., Mathieu, J., 1995. Ventilatory and locomotory activities in anoxia and subsequent recovery of epigean and hypogean crustaceans. Comptes rendus de l'Académie des sciences. Série III, Sciences de la vie 318, 585–592.

Jager, T., Albert, C., Preuss, T.G., Ashauer, R., 2011. General Unified Threshold Model of Survival - a Toxicokinetic-Toxicodynamic Framework for Ecotoxicology. Environ. Sci. Technol. 45, 2529–2540. https://doi.org/10.1021/es103092a

Jenny, J.-P., Francus, P., Normandeau, A., Lapointe, F., Perga, M.-E., Ojala, A., Schimmelmann, A., Zolitschka, B., 2016. Global spread of hypoxia in freshwater ecosystems during the last three centuries is caused by rising local human pressure. Global Change Biology 22, 1481–1489. https://doi.org/10.1111/gcb.13193

Kerr, J.L., Baldwin, D.S., Whitworth, K.L., 2013. Options for managing hypoxic blackwater events in river systems: A review. Journal of Environmental Management 114, 139–147. https://doi.org/10.1016/j.jenvman.2012.10.013

Klaus, J., McDonnell, J.J., 2013. Hydrograph separation using stable isotopes: Review and evaluation. Journal of Hydrology 505, 47–64. https://doi.org/10.1016/j.jhydrol.2013.09.006

Kunz, P.Y., Kienle, C., Gerhardt, A., 2010. Gammarus spp. in Aquatic Ecotoxicology and Water Quality Assessment: Toward Integrated Multilevel Tests, in: Whitacre, D.M. (Ed.), Reviews of Environmental Contamination and Toxicology Volume 205, Reviews of Environmental Contamination and Toxicology. Springer, New York, NY, pp. 1–76. https://doi.org/10.1007/978-1-4419-5623-1_1

Lee, X., Wu, H.-J., Sigler, J., Oishi, C., Siccama, T., 2004. Rapid and transient response of soil respiration to rain. Global Change Biology 10, 1017–1026.

Li, L., Sullivan, P.L., Benettin, P., Cirpka, O.A., Bishop, K., Brantley, S.L., Knapp, J.L.A., van Meerveld, I., Rinaldo, A., Seibert, J., Wen, H., Kirchner, J.W., 2021. Toward catchment hydro-biogeochemical theories. WIREs Water 8, e1495. https://doi.org/10.1002/wat2.1495

Lunardon, N., Menardi, G., Torelli, N., 2014. ROSE: a Package for Binary Imbalanced Learning. R Journal 6, 82–92.

Mallin, M.A., Johnson, V.L., Ensign, S.H., MacPherson, T.A., 2006. Factors contributing to hypoxia in rivers, lakes, and streams. Limnology and Oceanography 51, 690–701. https://doi.org/10.4319/lo.2006.51.1_part_2.0690

Maltby, L., 1995. Sensitivity of the crustaceans Gammarus pulex (L.) and Asellus aquaticus (L.) to short-term exposure to hypoxia and unionized ammonia: Observations and possible mechanisms. Water Research 29, 781–787. https://doi.org/10.1016/0043-1354(94)00231-U

McConnell, J.B., 1980. Impact of Urban Storm Runoff on Stream Quality Near Atlanta, Georgia. Municipal Environmental Research Laboratory, Office of Research and Development, U.S. Environmental Protection Agency.

McFadden, D., 1987. Regression-based specification tests for the multinomial logit model. Journal of econometrics 34, 63–82.

McGuire, K.J., McDonnell, J.J., 2010. Hydrological connectivity of hillslopes and streams: Characteristic time scales and nonlinearities. Water Resources Research 46. https://doi.org/10.1029/2010WR009341

Meijering, M.P.D., 1991. Lack of oxygen and low pH as limiting factors for Gammarus in Hessian brooks and rivers. Hydrobiologia 223, 159–169. https://doi.org/10.1007/BF00047637

Ministère chargé de l'écologie, 2019. Guide technique: relatif à l'évaluation de l'état des eaux de surface continentales (cours d'eau, canaux, plans d'eau).

Montuelle, B., Dorigo, U., Bérard, A., Volat, B., Bouchez, A., Tlili, A., Gouy, V., Pesce, S., 2010. The periphyton as a multimetric bioindicator for assessing the impact of land use on rivers: an overview of the Ardières-Morcille experimental watershed (France). Hydrobiologia 657, 123–141. https://doi.org/10.1007/s10750-010-0105-2

NSTC, 2003. An assessment of coastal hypoxia and eutrophication in US waters. National Science and Technology Council, Committee on Environment and Natural Resources.

Ockleford, C., Adriaanse, P., Berny, P., Brock, T., Duquesne, S., Grilli, S., Hernandez-Jerez, A.F., Bennekou, S.H., Klein, M., Kuhl, T., Laskowski, R., Machera, K., Pelkonen, O., Pieper, S., Smith, R.H., Stemmer, M., Sundh, I., Tiktak, A., Topping, C.J., Wolterink, G., Cedergreen, N., Charles, S., Focks, A., Reed, M., Arena, M., Ippolito, A., Byers, H., Teodorovic, I., 2018. Scientific Opinion on the state of the art of Toxicokinetic/Toxicodynamic (TKTD) effect models for regulatory risk assessment of pesticides for aquatic organisms. EFSA Journal 16, e05377. https://doi.org/10.2903/j.efsa.2018.5377

O'Donnell, B., Hotchkiss, E.R., 2022. Resistance and resilience of stream metabolism to high flow disturbances. Biogeosciences 19, 1111–1134. https://doi.org/10.5194/bg-19-1111-2022

Pardo, I., García, L., 2016. Water abstraction in small lowland streams: Unforeseen hypoxia and anoxia effects. Science of The Total Environment 568, 226–235. https://doi.org/10.1016/j.scitotenv.2016.05.218

Rabalais, N.N., Díaz, R.J., Levin, L.A., Turner, R.E., Gilbert, D., Zhang, J., 2010. Dynamics and distribution of natural and human-caused hypoxia. Biogeosciences 7, 585–619. https://doi.org/10.5194/bg-7-585-2010

Recoura-Massaquant, R., Martinache, P., Delorme, N., Chaumot, A., 2022. Experimental test of Gammarus fossarum sensitivity to hypoxic stress (No. Recherche Data Gouy, V1). INRAE.

Rode, M., Wade, A.J., Cohen, M.J., Hensley, R.T., Bowes, M.J., Kirchner, J.W., Arhonditsis, G.B., Jordan, P., Kronvang, B., Halliday, S.J., Skeffington, R.A., Rozemeijer, J.C., Aubert, A.H., Rinke, K., Jomaa, S., 2016. Sensors in the Stream: The High-Frequency Wave of the Present. Environ. Sci. Technol. 50, 10297–10307. https://doi.org/10.1021/acs.est.6b02155

Saari, G.N., Wang, Z., Brooks, B.W., 2018. Revisiting inland hypoxia: diverse exceedances of dissolved oxygen thresholds for freshwater aquatic life. Environ Sci Pollut Res 25, 3139–3150. https://doi.org/10.1007/s11356-017-8908-6

Samaniego, L., Thober, S., Kumar, R., Wanders, N., Rakovec, O., Pan, M., Zink, M., Sheffield, J., Wood, E.F., Marx, A., 2018. Anthropogenic warming exacerbates European soil moisture droughts. Nature Clim Change 8, 421–426. https://doi.org/10.1038/s41558-018-0138-5

Sarremejane, R., Cañedo-Argüelles, M., Prat, N., Mykrä, H., Muotka, T., Bonada, N., 2017. Do metacommunities vary through time? Intermittent rivers as model systems. Journal of Biogeography 44, 2752–2763. https://doi.org/10.1111/jbi.13077

Saup, C.M., H. Williams, K., Rodríguez-Freire, L., M. Cerrato, J., D. Johnston, M., J. Wilkins, M., 2017. Anoxia stimulates microbially catalyzed metal release from Animas River sediments. Environmental Science: Processes & Impacts 19, 578–585. https://doi.org/10.1039/C7EM00036G

Smith, V.H., Schindler, D.W., 2009. Eutrophication science: where do we go from here? Trends in Ecology & Evolution 24, 201–207. https://doi.org/10.1016/j.tree.2008.11.009

Sponseller, R.A., 2007. Precipitation pulses and soil CO2 flux in a Sonoran Desert ecosystem. Global Change Biology 13, 426–436.

Stanley, E.H., Fisher, S.G., Grimm, N.B., 1997. Ecosystem Expansion and Contraction in Streams. BioScience 47, 427–435. https://doi.org/10.2307/1313058

Strahler, A.N., 1957. Quantitative analysis of watershed geomorphology. Eos, Transactions American Geophysical Union 38, 913–920.

Therneau, T., Atkinson, B., 2022. rpart: Recursive Partitioning and Regression Trees.

Tramer, E.J., 1977. Catastrophic Mortality of Stream Fishes Trapped in Shrinking Pools. The American Midland Naturalist 97, 469–478. https://doi.org/10.2307/2425110

Uehlinger, U., 2000. Resistance and resilience of ecosystem metabolism in a flood-prone river system. Freshwater Biology 45, 319–332. https://doi.org/10.1111/j.1365-2427.2000.00620.x

Uehlinger, U., Naegeli, M.W., 1998. Ecosystem Metabolism, Disturbance, and Stability in a Prealpine Gravel Bed River. Journal of the North American Benthological Society 17, 165–178. https://doi.org/10.2307/1467960

Vannote, R.L., Minshall, G.W., Cummins, K.W., Sedell, J.R., Cushing, C.E., 1980. The River Continuum Concept. Can. J. Fish. Aquat. Sci. 37, 130–137. https://doi.org/10.1139/f80-017

Whitworth, K.L., Baldwin, D.S., Kerr, J.L., 2012. Drought, floods and water quality: Drivers of a severe hypoxic blackwater event in a major river system (the southern Murray–Darling Basin, Australia). Journal of Hydrology 450–451, 190–198. https://doi.org/10.1016/j.jhydrol.2012.04.057

Zarnetske, J.P., Bouda, M., Abbott, B.W., Saiers, J., Raymond, P.A., 2018. Generality of Hydrologic Transport Limitation of Watershed Organic Carbon Flux Across Ecoregions of the United States. Geophysical Research Letters 45, 11,702-11,711. https://doi.org/10.1029/2018GL080005

Zimmer, M.A., Kaiser, K.E., Blaszczak, J.R., Zipper, S.C., Hammond, J.C., Fritz, K.M., Costigan, K.H., Hosen, J., Godsey, S.E., Allen, G.H., Kampf, S., Burrows, R.M., Krabbenhoft, C.A., Dodds, W., Hale, R., Olden, J.D., Shanafield, M., DelVecchia, A.G., Ward, A.S., Mims, M.C., Datry, T., Bogan, M.T., Boersma, K.S., Busch, M.H., Jones, C.N., Burgin, A.J., Allen, D.C., 2020. Zero or not? Causes and consequences of zero-flow stream gage readings. WIREs Water 7, e1436. https://doi.org/10.1002/wat2.1436

765 **Supplementary**

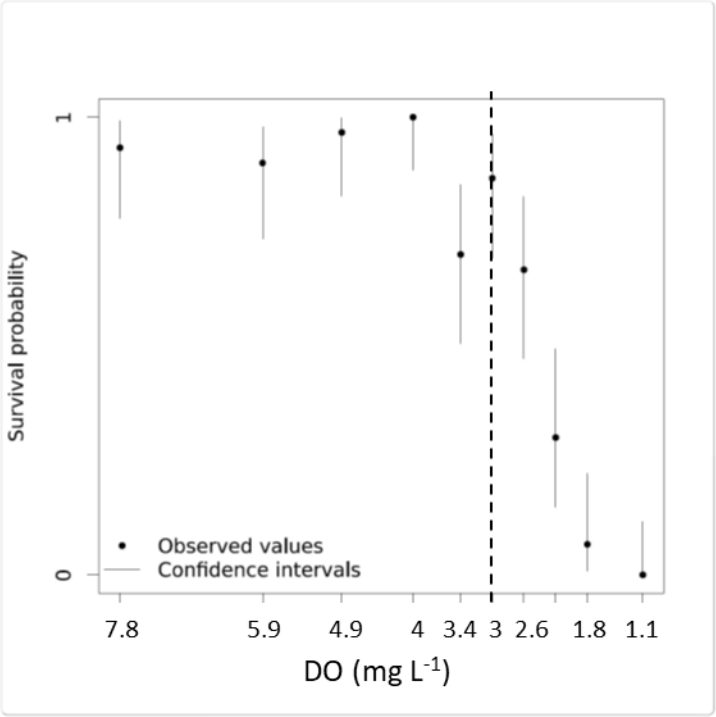

766

767 **Figure S1.** Five-day survival in the lab for the gammarids at varying levels of DO. Note the

768 survival threshold at approximately 3 mg L^{-1} (dashed vertical line). Experimental dataset:

769 doi.org/10.57745/KP9PO5

770

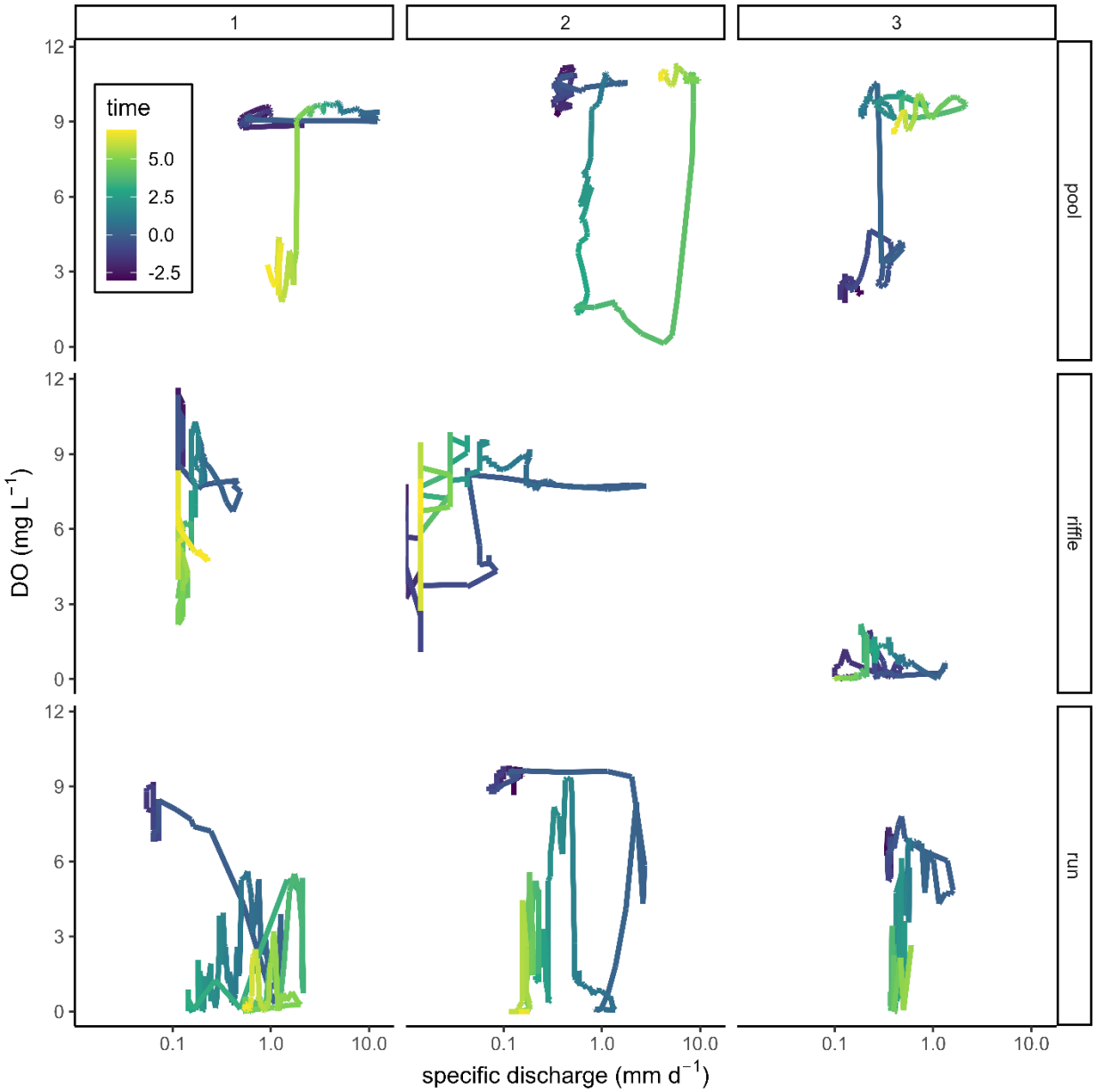

771

772 **Figure S2.** Hysteresis paths of DO versus q for the events shown in Figure 3 by unique storm

773 events (columns) and geomorphic habitat setting (rows) with color indicating the time relative to

774 peak storm discharge (days). Note the highly variable paths that DO takes across storm events.

Table S1. Hypoxia summary statistics by catchment, mean±sd when given.

Catchment	Hypoxia (hours)	Hypoxia (%)	Hypoxia (events)	Event length (hours)
Ardières	1844	2.5	31	18±28

Coise	3555	8.1	44	15±31
Lignon	1067	5.4	23	17±39
Loise	6110	5.9	37	12±21
Mare	1517	7.9	37	20±33
Toranche	2335	12.9	73	19±35
Vauxonne	57	0.3	9	6±5
Yzeron	296	0.3	7	8±8

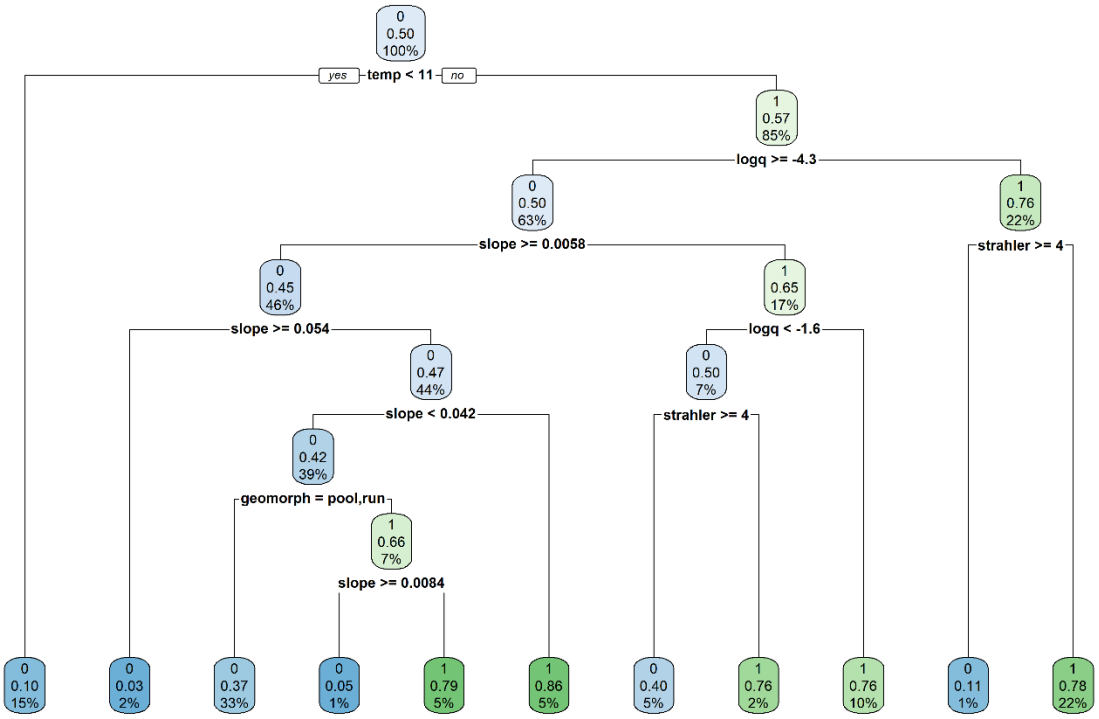

Figure S3. Classification tree for hypoxia (n = 266,079 from a balanced dataset). Each node shows from top to bottom: the predicted class (0 = oxic [blue], 1 = hypoxic [green]), the predicted probability of hypoxia, the percentage of total observations in the node.

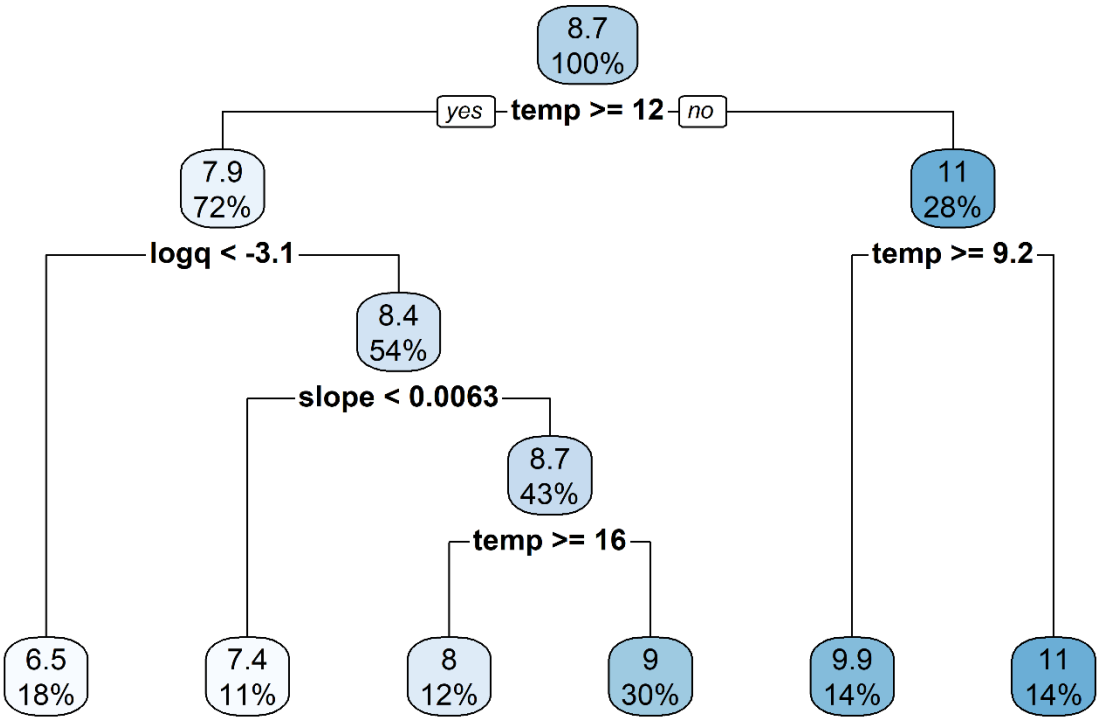

780

781 **Figure S4.** Regression tree for DO (n = 266,080 training data; 70%). Each node shows from

782 top to bottom: the predicted DO value (mg L^{-1}) and the percentage of total observations in the

783 node. Model details: based on testing data (n = 114032, 30%) RMSE = 1.8 mg L^{-1}, R^2=0.41,

784 MAE = 1.2 mg L^{-1}, bias = 0.0. Variable importances are temperature = 71, specific discharge =

785 21, slope = 7, Strahler order = 1, and light = 1.

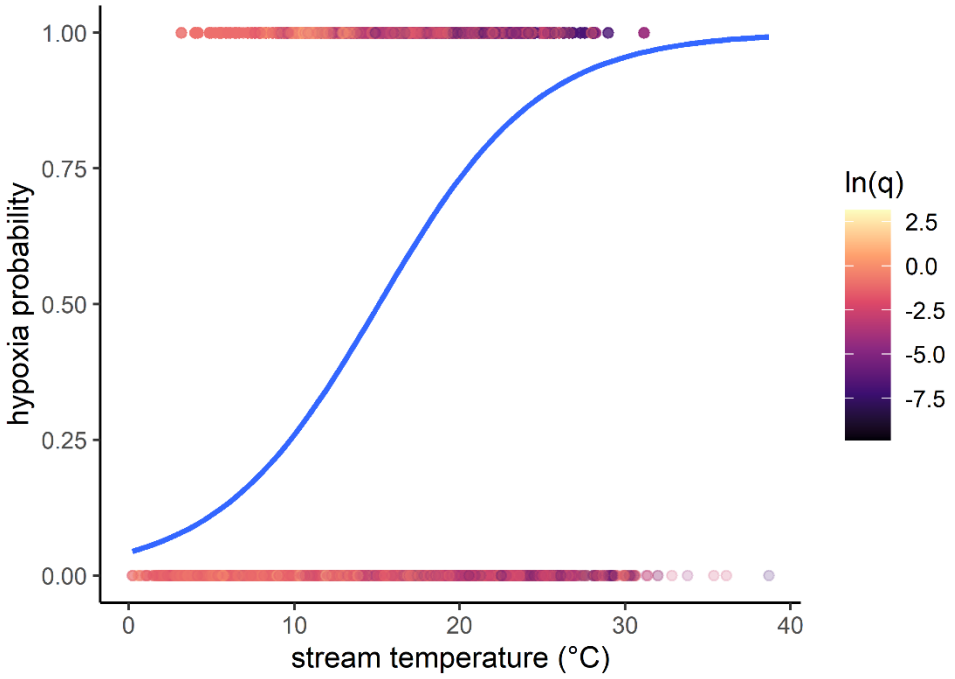

786

787 **Figure S5.** Logistic regression (blue line) of hypoxia on a balanced dataset of hypoxic and

788 oxic conditions (n=266,079) with point colors indication ln(specific discharge).